tomers, etc.), it is in harmony with the breadth of meaning implied by the etymology of the term as much as by its widespread usage in technological fields outside of chemistry, and, last but not least, it renders redundant and thus superfluous the term "configurational isomer", whose contradistinction to "conformational isomer" has saddled stereochemistry with a needless dichotomy.[45]
(44) Mislow, K. "Introduction to Stereochemistry"; W. A. Benjamin: New York, 1965; p 82.
(45) (a) A more detailed examination of these and related fundamental questions is reserved for future discussion. (b) For a different approach to the definition of "stereochemical configuration", see: Drozd, V. N.; Zefirov, N. S.; Sokolov, V. I.; Stankevich, I. V. *Zh. Org. Khim.* **1979**, *15*, 1785.
(46) The same absence of symmetry constraints or, expressed in physical terms, imbalance of bonding or nonbonding interactions is responsible for the pyramidality at other tricoordinate atoms whose "natural" ground state is planar. Calculations on carbocations amply bear this out. For example, the carbenium ion center in ethyl cation is pyramidal in a conformation in which a plane of symmetry bisects the H–C^+–H bond angle.[47] Similarly, the improbability of meeting the symmetry requirements for a planar ground state[17] is the underlying reason for pyramidality at the carbenium ion center in asymmetric tricyclic carbocations.[48]
(47) Lathan, W. A.; Hehre, W. J.; Pople, J. A. *J. Am. Chem. Soc.* **1971**, *93*, 808.
(48) Bach, R. D.; Siefert, J. H.; Tribble, M. T.; Greengard, R. A.; LeBel, N. A. *J. Am. Chem. Soc.* **1973**, *95*, 8182.
(49) Eliel, E. L. *Isr. J. Chem.* **1977**, *15*, 7.
(50) By extension of the same argument to other systems in the literature, it is easily seen that nonstereogenic chiral elements are widespread in organic chemistry. As in the present case, where such elements are centers they may have to be treated *as if* they were coplanar, a step which becomes necessary if the model of the molecule is to serve a useful function in the enumeration of stereoisomers. Of particular interest in this connection are two substituted biphenyls studied by Helmchen et al.,[51] biphenyl-2,2′,6,6′-tetracarboxylic acid tetra-(*S*)-α-phenylethylamide (D_2 symmetry) and 2′,6′-dimethoxycarbonylbiphenyl-2,6-dicarboxylic acid di-(*S*)-α-phenylethylamide (C_2 symmetry), neither of which has axial chirality since no permutation of the ligands on the biphenyl framework which maintains the constitution of the molecule can lead to stereoisomerism. However, although the chirality of these compounds is thus determined by the chirality of ligands and not by the chirality of the biphenyl moiety, the latter is expected to be chiral in the ground-state conformation of the molecule, on the basis of symmetry arguments similar to those adduced in connection with the chirality at nitrogen in **2**. A configurational descriptor (e.g., *P* or *M*, whichever applies) may therefore be attached to the biphenyl moiety in this compound. Nevertheless, since this moiety is not stereogenic, it may be treated as *if* it had local D_{2d} symmetry.
(51) Helmchen, G.; Haas, G.; Prelog, V. *Helv. Chim. Acta* **1973**, *56*, 2255.
(52) Lehn, J. M. *Top. Curr. Chem.* **1970**, *15*, 311. Rauk, A.; Allen, L. C.; Mislow, K. *Angew. Chem., Int. Ed. Engl.* **1970**, *9*, 400. Lambert, J. B. *Top. Stereochem.* **1971**, *6*, 19.
(53) An increase in the size of the ortho substitutents brings about an increase in the two-ring flip barrier,[20] and therefore also in the barrier to inversion at nitrogen.
(54) Germain, G.; Main, P.; Woolfson, M. M. *Acta Crystallogr., Sect. A* **1971**, *27*, 368.
(55) Gutowsky, H. S.; Jonas, J.; Siddall, T. H. III *J. Am. Chem. Soc.* **1967**, *89*, 4300.
(56) Laidler, K. J. "Chemical Kinetics", 2nd ed.; McGraw-Hill; New York, 1965; p 19.
(57) The transmission coefficient was assumed to be unity.

Photochemical Kinetics of Salicylidenaniline

P. F. Barbara, P. M. Rentzepis,* and L. E. Brus

Contribution from Bell Laboratories, Murray Hill, New Jersey 06974.
Received September 27, 1979

Abstract: The nanosecond and picosecond photochemical kinetics of quinoid fluorescence produced by excitation of the enol form of salicylidenaniline have been investigated in various environments. An excited state tautomeric proton transfer occurs within 5 ps at temperatures above 4 K in both protic and aprotic solvents. Bimodal fluorescence kinetics observed at low temperature appear to represent excited state vibrational relaxation occurring on the 10-ps time scale.

Introduction

The acidities of functional groups in excited electronic states are often strongly different than in ground electronic states. pK_a increases as large as 6 pK_a units have in fact been observed.[1] These large changes often induce proton-transfer reactions upon absorption of a photon. This type of photochemical reaction occurs in small molecules such as aromatic ketones[2] and fluorescent indicators,[3] as well as in complex biological systems such as rhodopsin.[4] In excited states, phenols, amines, and protonated amines usually become more acidic, while ketones, esters, carboxylic acids, amides, and azo groups become more basic.

The case where functional groups with opposite pK_a tendencies occupy nearby sites within one molecule is particularly interesting because the proton may move from one group to the other generating either transient or permanent tautomers of the original molecule. An example of this phenomenon is found in methyl salicylate (eq 1). Weller[5] first studied the

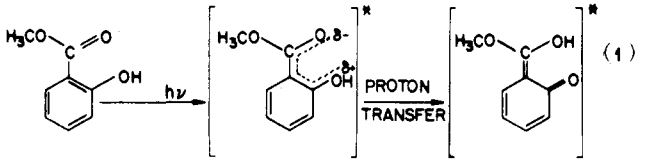

(1)

absorption and emission spectra of this compound, and concluded that the large fluorescence Stokes shift was the result of proton translocation. This proposal was supported by the absence of the unusually large Stokes shifted fluorescence in 2-methoxybenzoate. It was thought that a tautomer of the initially excited state[6,7] is generated as shown in eq 1. Recent work shows that the proton transfer is completed very rapidly without any evidence for a double minimum potential along the reaction coordinate in the excited state.[8,9]

Another class of compounds with similar proton-transfer properties are the salicylenanilines. These compounds have attracted much interest because of their additional ability to produce stable photochromic isomers of the initially colorless compound.[10-17]

This paper deals with the fluorescent properties of salicylidenaniline (**1**) and its derivatives, which exhibit very large

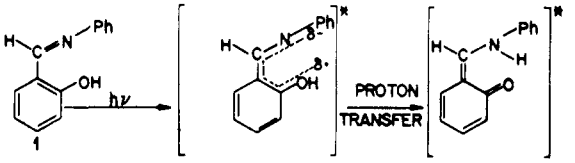

1

Stokes-shifted fluorescence.[14,15] Our purpose is to probe the excited state reaction dynamics of **1**, that is, to determine the time scale for excited-state proton transfer and to identify the intermediate species appearing before the photochromic species. The experimental techniques employed are time and wavelength resolved picosecond and nanosecond emission spectroscopy.

0002-7863/80/1502-2786$01.00/0

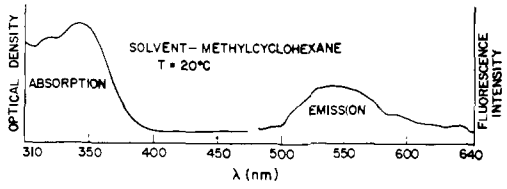

Figure 1. Absorption and emission spectra of a $\sim 10^{-4}$ M solution of **1** in methylcyclohexane.

Experimental Section

Absorption measurements (Figure 1) were made on a Cary 17 spectrometer. Time and wavelength resolved emission spectra were obtained with two experimental systems: (1) a low-temperature matrix nanosecond fluorescence system which has been described previously,[18] (2) a picosecond emission spectrometer that has been described in detail in a recent paper.[19] The nanosecond instrument consists of a frequency doubled, N_2 pumped dye laser ($\Delta t \simeq 3$ ns), a 1 M Chromatix monochromator, and a fast photomultiplier coupled with signal-averaging electronics. The picosecond apparatus is composed of (1) a Nd^{3+} mode-locked laser (6-ps pulse width) which generates a third harmonic 355-nm pulse from the laser fundamental at 1060 nm; (2) an Imacon 675 Photochon II streak camera capable of resolving ≤5 ps; (3) interference filters for spectral resolution. The optical streak image is digitized by a PAR 1205A optical multichannel analyzer, and subsequently processed on a Nova computer.

For the picosecond experiments, the experimental data consists of digital time resolved emission traces. In this paper, we have fitted the experimental data to computer-generated curves by a nonlinear least-squares procedure involving convolution to the experimental time dependence of the laser pulse.[19] This procedure, which is used to extract the actual time constants from the fluorescence, assumes a kinetic model in which the fluorescent state is created from the initially excited state by a first-order reaction having an inverse rate constant τ_r. In turn, the population of the fluorescent state is dissipated by a first-order decay with inverse rate constant τ_f. An experimental evaluation of the instrument has shown that τ_r as small as 5 ps can be resolved and that the accuracy in the measurement of τ_f is about 10%.[19]

Some of the fluorescence data presented in this paper (see Low-Temperature Fluorescence) could not be fitted adequately with a single pair of τ_r and τ_f. Therefore, a more complicated curve-fitting procedure was invoked which is described later.

The samples for the room temperature experiments were contained in 1-mm optical path length quartz cells. The low-temperature fluorescence was studied in frozen glass solutions and vapor deposited matrices. The low-temperature glass solution measurements were made in a 200-μm copper cell with quartz windows cooled by direct contact with a liquid He cryotip (Air Products, Inc.). Our matrix technique for deposition of large molecules (vapor pressure $\ll 10^{-3}$ Torr) has been recently described by Baca et al.[20] For both solution and matrix studies only front surface fluorescence was collected from samples of less than 200-μm thickness. Such thin samples produce negligible lifetime distortions.

Salicylidenaniline and its derivatives, **2-4**, were purchased from

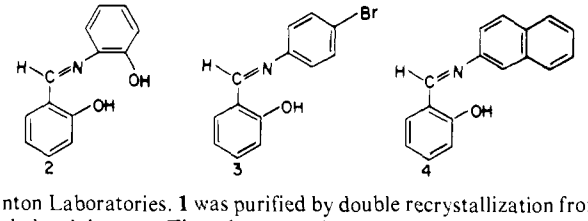

Frinton Laboratories. **1** was purified by double recrystallization from methylcyclohexane. The other materials were used without further purification. The solvents were either spectrograde (methylcyclohexane, 2-methylbutane, and *n*-pentane) or reagent grade (ether, methanol, and ethanol). The solution concentrations were $\sim 10^{-4}$ M.

Results

Room Temperature Fluorescence. Figure 1 shows the room temperature absorption and emission spectra of a $\sim 10^{-4}$ solution of **1** in methylcyclohexane. Both emission and absorption spectra in other nonpolar hydrocarbons, e.g., 2-methylbutane and *n*-pentane, were very similar to the spectra of Figure 1. These spectra are in good agreement with those observed in earlier studies.[14,15] The fluorescence maximum (540 nm, 18 158 cm^{-1}) is red shifted over 10 000 cm^{-1} from the absorption maximum (345 nm, 28 985 cm^{-1}). The origin of this emission has been previously assigned to the excited state keto tautomer of **1**, formed following absorption of a photon by the enol ground state.[14,15] The time dependence is presented in Figure 2a for a set of different average pulse energies. The peak intensity in time (see Figure 2b) was found to be related linearly to the average pulse energy throughout the range of energies used in this study.

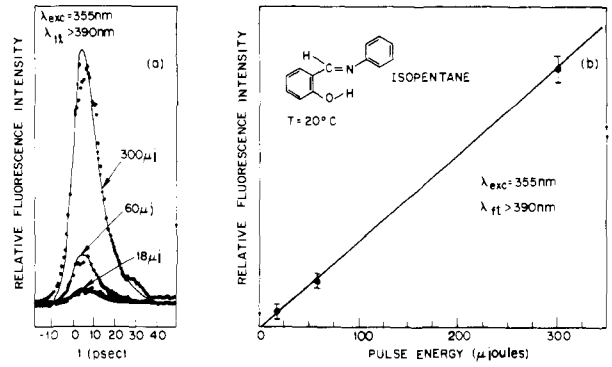

Figure 2. (a) The time-resolved fluorescence of a 10^{-4} M solution of **1** excited by a 355-nm excitation pulse. Each trace represents six laser pulses, and is fit by a computer-generated curve using $\tau_r = 0$ ps and $\tau_f = 8$ ps. (b) The energy dependence of the maximum intensity in the time-resolved fluorescence curves (six laser pulses per point). The beam was focused to a 4-mm spot on the sample cell.

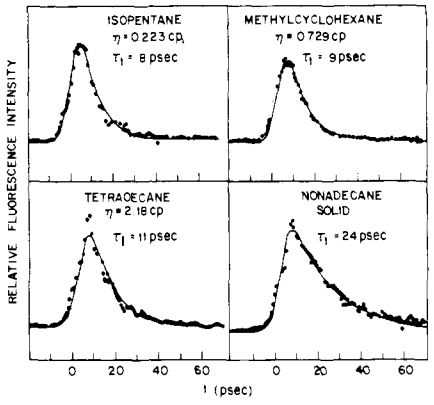

Figure 3. The time-resolved fluorescence ($\lambda_{fl} > 390$ nm) of **1** in various solvents. The computer-generated curves (solid lines) employ $\tau_r = 0$ ps in all cases. Each experimental trace is an average of ten 100-μJ laser pulses.

A computer fit of the time dependence indicates that the time constant for the rate of formation of the fluorescence state τ_r is ≤5 ps. The lifetime of the fluorescing state is 8 ± 2 ps. The same kinetics ($\tau_r \leq 5$ ps and $\tau_f = 8 \pm 2$ ps) are observed when the fluorescence was measured in narrow wavelength bands, $\Delta\lambda = 10$ nm, at 470, 480, 490, 500, 540, and 570 nm.

Experiment in solvents of widely varying viscosities, from 0.223 cP for 2-methylbutane to the solid environment of crystalline nonadecane, show that the fluorescence kinetics of **1** are only slightly affected; see Figure 3. The lifetime of the fluorescence, τ_f, increased by a factor of 3 for a $\sim 10^3$ increase in viscosity. Solvent polarity over a limited range also seems to have little effect as the kinetics in ether with dielectric constant 4.18 are indistinguishable from the kinetics in non-

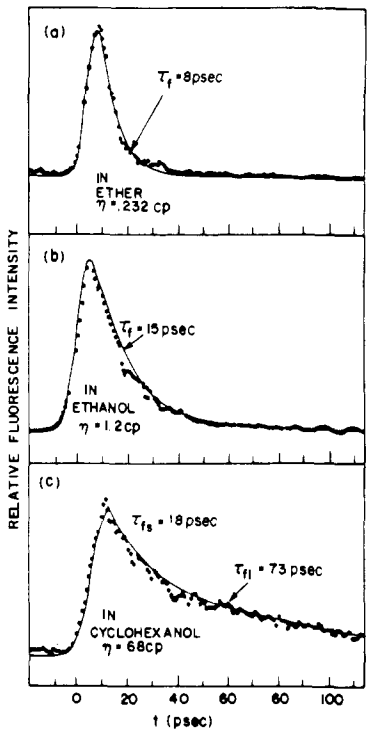

Figure 4. Time-resolved fluorescence (λ_{fl} >390 nm) of **1** in various solvents. Each experimental curve is an average of ten 100-μJ laser pulses. The computer-generated curves are based on τ_r = 0 ps.

Table I. Fluorescence Decay of SA Derivative

compd	solvent	
	τ_{EtOH}, ps	$\tau_{methylcyclohexane}$, ps
1	15	8
2	40	8
3	15	7.5
4	22	10

Table II. Fluorescence Decay of SA

solvent	τ_f, ps	solvent	τ_f, ps
MeOH	12	EtOD	14
MeOD	13	ether-10% MeOH	9
EtOH	15	ether-10% MeOD	8

polar hydrocarbons such as 2-methylbutane, with a dielectric constant of 2.02.

In the case of protic solvents, however, as shown in Figures 4b and 4c, τ_f is found to be significantly longer; i.e., τ_f = 15 ps for ethanol while τ_r remains <5 ps. In cyclohexanol, a more viscous protic solvent, the fluorescence exhibits a biexponential decay, which is independent of emission wavelength in the range 490-570 nm, with a short decay component τ_{fs} = 28 ps and a long τ_{fl} = 73 ps. In this case there may be two solvated forms of **1** in the excited state.

The kinetics of **2–4** were similar to that of **1** as shown in Table I. For **1–4** the rise time of the fluorescence (τ_r) is measured to be <5 ps, and τ_f in methylcyclohexane is 8-10 ps. For **1, 3,** and **4,** dissolved in ethanol, τ_f was found to be twice as long as in methylcyclohexane; however, τ_f is five times longer for **2** in EtOH than when dissolved in methylcyclohexane.

Deuterium substitution of the phenolic proton on **1** had a negligible effect on the room temperature fluorescence kinetics, as indicated in Table II by the virtually unchanged fluorescence lifetime in deuterated protic solvents and mixtures of aprotic and protic solvents. In both cases the labile phenolic proton of

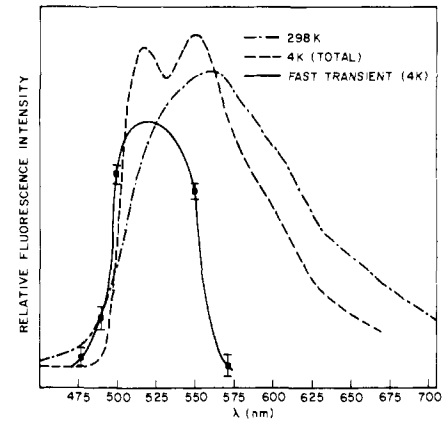

Figure 5. (-·-) and (- - -) are time-unresolved fluorescence spectra of **1**, ether solvent, at 298 and 4 K, respectively. (—) is the fluorescence spectrum of component A based on a calculation using the low-temperature time- and wavelength-resolved fluorescence; see text.

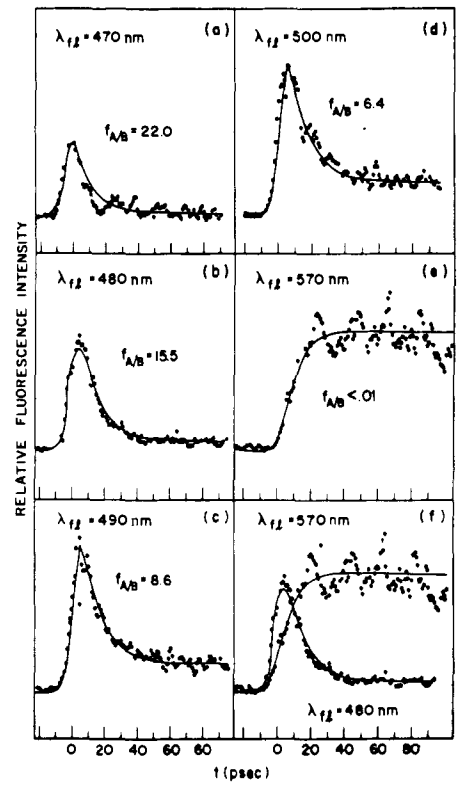

Figure 6. (a-e) Time- and wavelength-resolved fluorescence curves for **1** in frozen ether solution at 4 K. Wavelength regions were selected by insertion of narrow-band ($\Delta\lambda$ = 10 nm) interference filters in the fluorescence collection optics. Each curve is an average of 20 400-μJ laser pulses. (f) A composite plot of (e) and (b).

1 (10^{-4} M) is entirely deuterated by exchange with the solvent.

Low-Temperature Fluorescence. A. Bimodal Kinetics. Low-temperature fluorescence measurements of **1** were made in frozen solution of various organic solvents and vapor-deposited matrices of ether, argon, and xenon. The 10 K total emission spectrum of **1** in ether matrix, Figure 5, shows slightly better vibrational resolution and a sharper blue edge than the room temperature spectrum. The fluorescence kinetics of **1** at low temperatures are very different from those at room temperature, however, and are strongly dependent on emission wavelength, as shown in Figure 6. On the short-wavelength edge of the fluorescence (470 nm) a transient behavior can be identified with τ_r < 5 ps and τ_f = 10 ps, which we label as

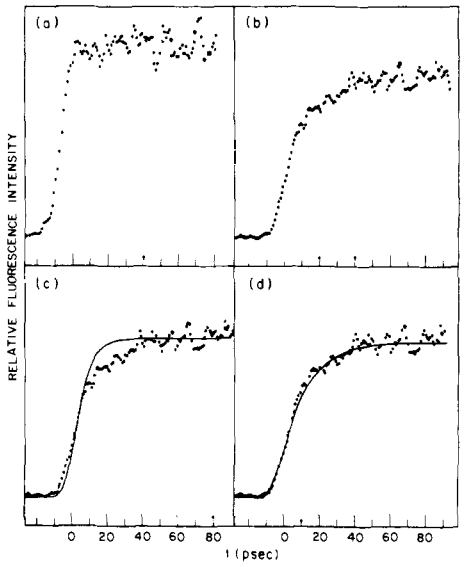

Figure 7. (a) The instrument-limited rise time, i.e., the time-resolved fluorescence of a dilute solution of coumarin dye (fluorescence lifetime >3 ns) excited by 100-μJ 355-nm pulses. (b) Experimentally observed fluorescence in the λ >500 nm region for **1** in ether. (c) The same data as (b) except fitted by a simulated curve using τ_r = 5 ps and τ_f = 5000 ps. (d) The same data as (b) except fitted by a composite ($f_{A/B}$ = 0.2) of components A and B; see text.

component A. The long-wavelength fluorescence component B at 570 nm shows an entirely different behavior, τ_r = 10 ps and $\tau_f \simeq$ 3 ns. At intermediate wavelengths the kinetics are complicated and cannot be adequately assigned to a single rise time (τ_r) and fall time (τ_f). They are, however, well represented by a varying mixture of transient mixture A and long B components. The A to B ratio found in the computer-generated curves is denoted by $f_{A/B}$ in Figure 6.

The bimodal nature of the fluorescence rise time (τ_r) is particularly evident for emission in the λ >500 nm region. Figure 7b shows a comparison of this bimodal rise time with an experimental pulse limited rise time. The observed fluorescence for **1** clearly shows a rise time which cannot be adequately simulated with a single value for τ_r (see Figure 7c). However, a composite fit of components A and B does reproduce the observed kinetics, as Figure 7d illustrates.

The similarity of the decay of component A, τ_f = 9 ± 2 ps, and the rise time of component B, τ_r = 11 ± 2 ps, strongly suggests that the *species responsible for component A is the kinetic precursor to the species responsible for component B.* Further experiments establishing that A and B are sequential transient excited states within the same molecule are described in following paragraphs. Since the decay lifetime of A is 9 ± 2 ps and the decay of B is orders of magnitude longer, it is reasonable to assume that the total fluorescence originates entirely from component B.

An approximate spectrum for component A can be constructed from the A to B ratios (Figure 6) and the total emission spectrum. This procedure requires that component B dominate the total emission spectrum at wavelengths longer than 470 nm. The spectrum of component A shown in Figure 5 is the prompt (<5 ps) fluorescence of **1** in ether at 4 K. Compared with the component B spectrum, the A spectrum is narrower and shifted to the blue.

We find that the fluorescence kinetics are not appreciably affected by a change in solvent. Similar A and B bimodal behavior was also observed in a frozen solution of *n*-pentane and 20% 2-methylbutane in methylcyclohexane. The fluorescence kinetics in vapor-deposited 4 K matrices of argon, ether, and xenon depicted in Figure 8 were also very similar to those presented in Figures 5 and 6.

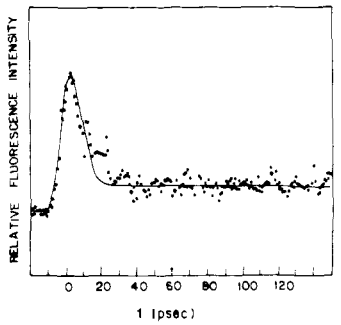

Figure 8. Time-resolved fluorescence (400–500 nm) at 4 K of a vapor-deposited xenon matrix of **1**. The computer-generated curve is essentially a composite fit of components A and B. The data are an average of ten 400-μJ laser pulses.

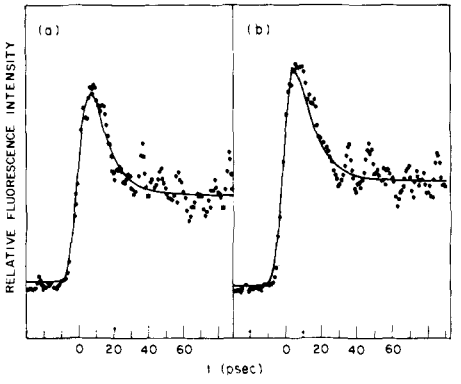

Figure 9. Time-resolved fluorescence (400–500 nm) at 4 K for dilute solutions of **1** in ether with 5% added MeOH (a) and MeOD (b). The experimental data, which are an average of ten 300-μJ laser pulses, are fit in both curves by the same composite of components A and B.

B. Deuterium Substitution. In order to determine the hydrogen/deuterium isotope effect on the A and B bimodal kinetics, the time-resolved fluorescence was measured for samples of **1** (10^{-4} M in ether) with added 5% MeOH or 5% MeOD. In the MeOD sample the phenolic protons of **1** should be entirely exchanged. The fluorescence kinetics for both the protonated and deuterated samples (Figures 9a,b) are adequately modeled by the same composite A and B kinetic scheme. Within the precision of these experiments, a *kinetic hydrogen/deuterium isotope effect was not observed.*

C. Excitation Pulse Intensity Dependence. If both A and B components occur following absorption of only one photon, then both would show a linear dependence on excitation pulse intensity in the absence of saturation. The measured fluorescence intensity dependence on excitation energy in the range of 0.1–1.5 mJ/pulse is linear for both A and B components. This is clearly shown in Figure 10, where the open circles correspond to the intensity of the fluorescence maximum at 5 ps which is predominantly due to component A and the solid circles are the intensities at 75 ps belonging predominantly to component B. We conclude therefore that neither component originates from a nonlinear optical process.

D. Alternate Kinetic Hypothesis. A possible complication is the presence of a trace amount of second ground-state isomer **Q1**, a *cis* keto form that also absorbs in the same region and

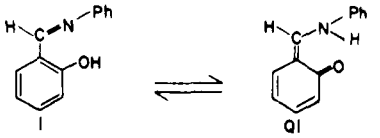

subsequently fluoresces, eq 3. One might hypothesize that component A is the **Q1** fluorescence. **Q1** has an absorption maximum at 440 nm (shifted ~80 nm to longer wavelengths

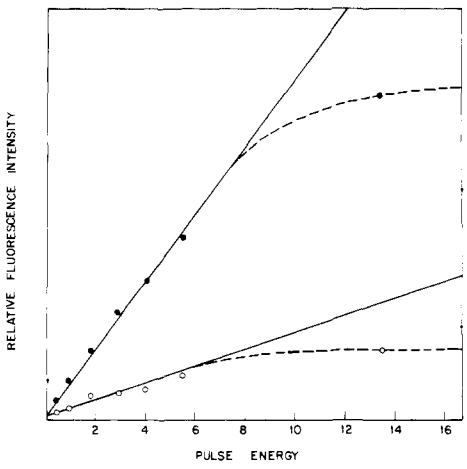

Figure 10. The fluorescence intensity in the 400–500 nm region for a 4 K solution of **1** in ether as a function of excitation pulse energy for 0 (○) and 75 ps (●) in the time-resolved experiments. One unit on the arbitrary energy scale corresponds to about 100 μJ of 355-nm excitation. (—), linear dependence on excitation energy; (- - -), saturating.

than **1**).[14,15] It has been shown—and reproduced in our nanosecond experiments for **1** in argon matrix—that the fluorescence spectrum of **Q1** when excited at ~440 nm is slightly yet reproducibly different from that of **1** excitation at ~340 nm.[21]

We have demonstrated in our nanosecond experiments that it is possible to bleach photochemically the **Q1** fluorescence entirely in a 4 K argon matrix of **1**, by irradiating at 440 nm for extended periods. This bleaching, however, does not lower detectably the amount of **1** present, because we observe that the total fluorescence intensity after excitation of **1** at 365 nm is unaffected by earlier bleaching at 440 nm. Therefore, it is possible to prepare argon matrix samples with **1** and **Q1** present in their 300 K relative proportions, or samples with **1** present but **Q1** absent because of bleaching. We observe that the picosecond bimodal kinetics are unaffected by photobleaching at 440 nm, which proves that neither component A nor B results from excitation of the trace isomer **Q1**.

A further possible complication involves formation of dimers and/or aggregates in slowly frozen solutions. One might interpret the A component, which appears at low temperature, as due to aggregates of **1**. In matrix-deposited samples, however, aggregate formation should be entirely suppressed. As the A and B components have the same relative proportion in frozen solutions of ether as in ether matrices, we conclude that the A and B components both are emission in monomer species.

Discussion

Our data show that the fluorescence of **1**, irradiated with a 355-nm picosecond pulse, is composed of two resolvable components. The initially formed species is component A, which appears with a pulse limited rise time, and is rapidly converted (10 ps in ether) into component B. Since the latter species' lifetime is 500 times longer than that of the former, the total emission spectrum is dominated by the longer lived species; the <5 ps fluorescence is primarily composed of emission by the shorter lived species. Since both species have fluorescence spectra that are substantially Stokes shifted from a possible enol mirror image fluorescence, we believe that both A and B represent quinoid forms of **1**. The dominant B component has been previously assigned to a vibrationally relaxed, electronically excited cis keto quinoid tautomer.[14,15] For this discussion, the short-lived state is labeled QA*, while the vibrationally relaxed state is labeled QB*.

The rate of proton transfer is given by the rise time of the quinoid fluorescence. Analysis of the room temperature fluorescence of **1** reveals a pulse limited rise time (<5 ps) at all wavelengths studied in a broad range of aprotic and protic solvents. Furthermore, the rise time is still as short when the transferring proton is replaced by a deuteron. At low temperatures, component A has a <5 ps rise time in all the experimental conditions studied, including deuterium substitution of the phenolic proton. The 355-nm absorption produces excited molecules **1*** near the vibrational origin of the enol excited state. If we envision a one-dimensional reaction coordinate model for the tautomeric proton transfer, then any possible barrier to proton transfer must be very small. In view of the unresolved proton transfer time constant (<5 ps) and the absence of an isotope and temperature effect, we cannot eliminate an activated or tunneling proton translocation process involving a very small barrier.

The kinetic data and fluorescent spectra of QA and QB offer little direct evidence on the structural properties of these states. The following discussion outlines one possible assignment which is consistent with our kinetic data as well as previously published experimental data relating to the photochemistry of **1**.

The ultimate photoproduct of **1** is the ground-state photochromic species, which absorbs in the 500–550-nm region. This component, labeled QC, is believed to be an additional quinoid isomer of **1** but not the same species as Q1. It has been observed that the yield of QC produced on irradiation of **1** is inversely related to the yield of fluorescence, and varies with temperature.[17] At higher temperatures the fluorescence is weak but the yield of QC relatively high. At low temperatures, however, the yield of the fluorescence increases and the yield of QC decreases. Furthermore, QB* cannot be a kinetic precursor of QC since it has been observed that the ratio of yields of fluorescence to that of photoproduct QC is strongly dependent on the excitation wavelength. To explain these results, Ottolenghi and co-workers[17] proposed that the common precursor to QC and to QB* is a vibrationally excited state of QB*. Our data are consistent with this proposal and we tentatively assign QA* as Ottolenghi's vibrationally excited QB* state. The absence of an isotope effect appears to imply that the relaxation process we observe does not involve the acidic proton.

This model is presented in Scheme I. The Franck-Condon vertically excited enol state **1** undergoes a tautomeric proton transfer producing QA*, which contains a substantial amount of excess vibrational energy. The excited state QA* is reactive toward formation of QC, and also is rapidly converted to relaxed QB* by vibrational relaxation. The related QB*, however, does not produce QC. This model is also consistent with the room temperature fluorescence kinetics we observed, if it is assumed that QA* in interconverted to QB* in a time faster than 5 ps. This assumption is quite reasonable for a large molecule in solution, and would explain the short rise time at all wavelengths. Subsequent thermal activation of QB* could explain the short room temperature τ_f.

Conclusions and Summary

The time- and wavelength-resolved fluorescence of **1** and its derivatives has been investigated in a variety of environments and temperature. It is observed that the quinoid fluorescence produced by excitation of the enol form at room temperature has a <5 ps rise time which is consistent with a $\geq 2 \times 10^{11}$ s^{-1} rate for tautomeric proton transfer. At low temperatures, the fluorescence was found to have two components: a short-lived component which is formed within 5 ps of excitation, and a long-lived component which has the short-lived fluorescent state as a precursor. Deuterium substitution was found to have no effect on the observed kinetics.

This behavior has been interpreted as a very rapid proton-transfer process occurring at all temperatures. The short-lived

Scheme I. Simplified Schematic Representation of a Possible Photoisomerization Mechanism as Described in the Text[a]

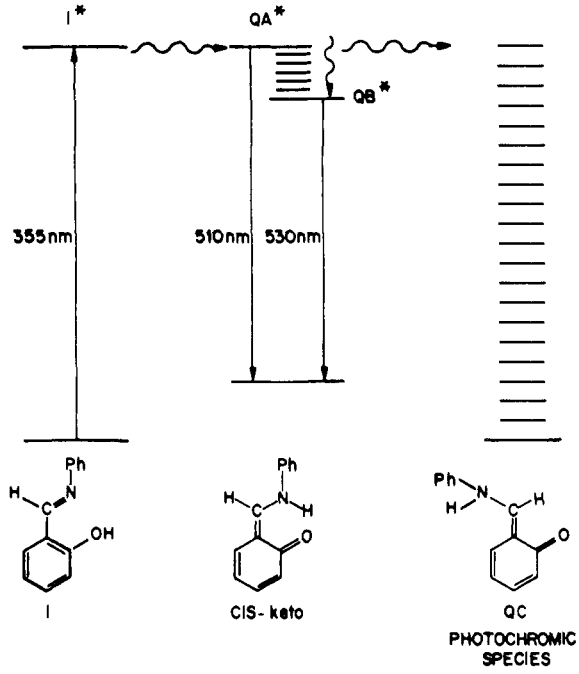

[a] As discussed in ref 17, each of the labels 1, cis keto, and QP may actually represent several kinetically distinct conformers. QA* and QB* denote respectively vibrationally excited and vibrationally relaxed forms of the electronically excited "cis keto" molecule.

component of the fluorescence, which is blue shifted from the long-lived fluorescence, has tentatively been assigned to vibrationally excited fluorescence. This interpretation is consistent with the previously determined excitation wavelength dependence of the yield of fluorescence and photochromic species.[17] Several experiments are being planned to elucidate further the photochemical reaction mechanism. A systematic investigation of the bimodal fluorescence, as well as picosecond absorption studies, will be performed.

Our tentative assignment of vibrationally unrelaxed ("hot") fluorescence in such a large molecule is quite unusual and interesting. It may be that the "vibrational relaxation" we observe is torsional relaxation about the C_1-C_7 bond. Very little is known about internal vibrational redistribution, and/or vibrational and torsional energy transfer to the environment, in molecules of this size. Potentially, a thorough study of vibrationally excited fluorescence should lead to a better understanding of these phenomena. In reacting systems, these studies may lead to a better understanding of reactions driven by excess vibrational energy.

References and Notes

(1) W. Klopffer, *Adv. Photochem.*, **10**, 311 (1977).
(2) E. van der Donckt, *Prog. React. Kinet.*, **5**, 273 (1970).
(3) A. Weller, *Prog. React. Kinet.*, **1**, 188 (1961).
(4) K. Peters, M. L. Applebury, and P. M. Rentzepis, *Proc. Natl. Acad. Sci. U.S.A.*, **74**, 3119 (1977).
(5) A. Weller, *Naturwissenschaften*, **42**, 175 (1955); *Z. Elektrochem.*, **60**, 1144 (1956).
(6) E. M. Kosower and H. Dodiuk, *J. Lumin.*, **11**, 249 (1975).
(7) W. Klopffer and G. Naundorf, *J. Lumin.*, **8**, 457 (1974).
(8) J. Goodman and L. E. Brus, *J. Am. Chem. Soc.*, **100**, 7472 (1978).
(9) K. K. Smith and K. J. Kaufman, *J. Phys. Chem.*, **82**, 2286 (1978).
(10) M. D. Cohen and G. M. J. Schmidt, *J. Phys. Chem.*, **66**, 2442 (1962).
(11) M. D. Cohen and S. Flavian, *J. Chem. Soc. B*, 317, 321, 334 (1967).
(12) D. G. Anderson and G. Wettermark, *J. Am. Chem. Soc.*, **87**, 1433 (1965).
(13) M. Ottolenghi and D. S. McClure, *J. Chem. Phys.*, **46**, 4620 (1967).
(14) R. S. Becker and W. F. Richey, *J. Am. Chem. Soc.*, **89**, 1298 (1967).
(15) W. F. Richey and R. S. Becker, *J. Chem. Phys.*, **49**, 2092 (1968).
(16) P. Potashnik and M. Ottolenghi, *J. Chem. Phys.*, **51**, 3671 (1969).
(17) T. Rosenfeld, M. Ottolenghi, and A. Y. Meyer, *Mol. Photochem.*, **5**, 39 (1973).
(18) J. Goodman and L. E. Brus, *J. Chem. Phys.*, **65**, 1156 (1976).
(19) P. F. Barbara, L. E. Brus, and P. M. Rentzepis, *Chem. Phys. Lett.*, in press.
(20) A. Baca, R. Rossetti, and L. E. Brus, *J. Chem. Phys.*, **70**, 4475 (1979).
(21) This observation shows that the cis keto isomer **Q1** does not have the same conformation as the excited cis keto isomer produced by excitation of the enol. As shown in reference 17, a large number of keto and enol conformations of **1** are actually possible.

Photolysis of the Endoperoxide of Heterocoerdianthrone. A Concerted, Adiabatic Cycloreversion Originating from an Upper Excited Singlet State

R. Schmidt, W. Drews, and H.-D. Brauer*

Contribution from the Institute for Physical and Theoretical Chemistry, University of Frankfurt, D-6000 Frankfurt/M. 1, West Germany.
Received September 6, 1979

Abstract: In the present work we report the photolysis of the endoperoxide (PO) of heterocoerdianthrone (HCD = dibenzo[*aj*]-perylene-8,16-dione). Two different photoreactions were observed: (1) an irreversible decomposition of PO, whose reaction products were not analyzed (this reaction occurs with a quantum yield of $Q_{dec} = 0.006$ either from the $S_1(n,\pi^*)$ state or, more probably, from the $T_1(n,\pi^*)$ state); (2) a photoreversible cleavage of PO into HCD and O_2 (this reaction originates from the $S_2(\pi,\pi^*)$ state with a maximum quantum yield of $Q_1 = 0.26$). Only the very rapid internal conversion from $S_2(\pi,\pi^*)$ to $S_1(n,\pi^*)$ competes with this photoreaction. The products of the photocleavage are HCD in its ground state and O_2 in an electronically excited singlet state. These results confirm for the first time the predictions made by Kearns and Khan on the basis of state correlation diagrams concerning the concerted photocleavage of endoperoxides.

Introduction

In a recent article we introduced a new photochromic system which is based on the photoreversible addition of $O_2(^1\Delta_g)$ into an arene derivative.[1] The colored component is the red-violet heterocoerdianthrone (HCD = dibenzo[*aj*]perylene-8,16-dione). Self-sensitizing photooxidation of HCD leads to the formation of endoperoxide (PO), which in our photochromic

0002-7863/80/1502-2791$01.00/0